

# Studies of Nuclei Far from the Stability Line with Macro-Microscopic Model

Zheng Chunkai, Hu Jimin, and Xu Fulong

(Department of Technical Physics, Peking University, Beijing, China)

The macro-microscopic model is applied to study the properties of the nuclei far from stability line. Some results are obtained, e.g., proton and neutron drip line, changes of proton and neutron density distributions, and the rms radii and neutron skin thickness with isospins. The calculated results of some exotic nuclei are compared with those of relativistic mean-field approach. Brief discussions for proton radioactivity are given.

**Key words:** macro-microscopic model, nuclear properties far from stability line, drip line, density distribution, rms radii.

---

## 1. INTRODUCTION

Properties of nuclei far from the  $\beta$ -stability line are one of the most interesting problems in nuclear structure studies. For example, the limits of proton number  $Z$  and neutron number  $N$  for the possible formation of a nucleus are to be determined as proton and neutron drip lines. Essential properties of nuclei far from the  $\beta$ -stability line, such as proton and neutron densities, change of the rms radii along the isotopic or isotonic lines and other exotic properties are to be studied experimentally and theoretically. Light radioactive beams are available at present and heavier beams are in the project of several laboratories. Studies of the properties of the nuclei far from the  $\beta$ -stability line are under way. In our country, important achievements have been made in the synthesis of new

---

Received on February 8, 1995. Supported by the National Natural Science Foundation of China and the Foundation from the Ph.D. Program of High Education of China.

© 1996 by Allerton Press, Inc. Authorization to photocopy individual items for internal or personal use, or the internal or personal use of specific clients, is granted by Allerton Press, Inc. for libraries and other users registered with the Copyright Clearance Center (CCC) Transactional Reporting Service, provided that the base fee of \$50.00 per copy is paid directly to CCC, 222 Rosewood Drive, Danvers, MA 01923.

neutron rich nuclides and further studies are in progress. New results in the studies of properties of neutron deficit nuclei (near the proton drip line) are obtained. It is both necessary and meaningful to study theoretically the properties of nuclei far from the  $\beta$ -stability line.

We have proposed a macroscopic model based on the energy functional of the nuclear system [1]. It has been applied successfully to study the properties of the ground states [2], deformed states [3], and high-spin states [4] of the known nuclei. Good results have been obtained from the mass formula of this model with the microscopic corrections given by Möller and Nix [5]. In this paper, we shall apply this model to study properties of nuclei far from the  $\beta$ -stability line, with microscopic corrections for certain problems.

## 2. NUCLEAR MACRO-MICROSCOPIC MODEL

In our macroscopic model, it is assumed that the energy of the nucleus can be expressed as the following functional of the neutron density  $\rho_n$  and the proton density  $\rho_p$ ,

$$\begin{aligned}
 E[\rho_n, \rho_p] = & \int [-a_1 + a_3(\rho_n - \rho_p)^2 / \rho_s^2 + sa_3(\rho_n + \rho_p - \rho_s)^2 / \rho_s^2] \rho_s dV \\
 & + \int [a_4 - a_6(\rho_n - \rho_p)^2 / \rho_s^2 + sa_6(\rho_n + \rho_p - \rho_s)^2 / \rho_s^2] \varphi \rho_s dV \\
 & + \frac{e^2}{2} \iint \frac{\rho_p(\mathbf{r}_1) \rho_p(\mathbf{r}_2)}{|\mathbf{r}_1 - \mathbf{r}_2|} dV_1 dV_2,
 \end{aligned} \quad (1)$$

where  $a_1$ ,  $a_3$ ,  $a_4$ ,  $a_6$ , and  $s$  are adjustable parameters, and  $\rho_s$  is the reference density, which may take the form

$$\rho_s = \frac{t}{4\pi a^3} \{1 + \exp[(r / \lambda f - R_0) / a]\}^{-1}, \quad (2)$$

$$\varphi = |\nabla \rho_s| / \rho_s, \quad (3)$$

In formula (2),  $R_0$  can be determined from the condition

$$\int \rho_s dV = A$$

For axisymmetrical deformations,  $f = f(\theta)$ ,

$$f(\theta) = 1 + \sum_{n=2}^{\infty} \alpha_n P_n(\cos \theta). \quad (4)$$

Variation of  $\rho_n$  and  $\rho_p$ , and minimizing the functional (1), the proton density, neutron density, and the ground state energy can be determined. Therefore, the average properties related to the density distributions, such as the rms proton radius, neutron radius, and Coulomb energy can be calculated. With a few additional terms and microscopic corrections (shell and pairing corrections), the mass formula for the ground state is obtained. If rotational energy is added to functional (1), properties of rotational nuclei can be studied.

With a macroscopic model, only the average properties of the nucleus can be studied. In some cases, it is necessary to incorporate the microscopic corrections to obtain satisfactory results. Microscopic corrections to nuclear energy include shell and pairing corrections [5,6]. Möller and Nix have made detailed studies of these corrections. For shell corrections, they have chosen the folding Yukawa potential as the average field. The advantage of such a choice is that the potential behaves correctly even for very large deformations, but considerably more amount of calculations are involved. For the ground state studies, no large deformations are involved, therefore we have chosen the Nilsson potential with stretching coordinates [7]. With such a potential, it is easier to adjust the parameters to obtain the best microscopic corrections. For pairing corrections, Möller and Nix used the Lipkin-Nogami model [6], which can approximately satisfy the particle number conservation. It is an improvement over the usual BCS model, but with a much larger amount of calculations. To simplify calculations, we have used the usual BCS model, although larger errors may be involved for light nuclei. In this way, we have established a set of simplified microscopic corrections, which is combined with our macroscopic model to form the macro-microscopic model for nuclear structure studies. Preliminary results indicate that the ground state masses calculated with this model are still in good agreement with the empirical data [7].

The parameters in our model can be determined by fitting the measured nuclear masses, proton density distributions, and the rms proton radii with the following results:  $t = 0.3$ ,  $a = 0.5220$  fm,  $a_1 = 16.1650$  MeV,  $a_3 = 27.012$  MeV,  $a_4 = 15.147$  MeV,  $a_1/a_3 = 0.55$ , and  $s = 0.4770$ . The physical significance of these parameters are:  $a$  is the thickness of the diffuse layer of the nucleus,  $t$  is connected to the nuclear density in the central region,  $t/(4\pi a^3)$ ,  $a_1$  is the volume energy per nucleon,  $a_3$  and  $a_6$  are the volume and surface coefficient of symmetrical energy  $a_4$  is the surface energy coefficient, and  $sa_3$  and  $sa_6$  are the volume and surface coefficient of compressibility energy. With this set of parameters, together with some other fixed minor corrections (Wigner energy, odd and even correction, and Coulomb exchange correction), the nuclear properties of the known nuclei can be reproduced with the following results: nuclear masses (for 1500 known nuclear masses, with rms deviations 0.8 MeV), rms proton radii (for 256 measured radii, with rms deviations 0.03 fm), Coulomb energy differences between isotope analogue states (for 210 pairs with average deviation 0.15 MeV), and proton distributions of spherical and deformed nuclei (good agreements are obtained for all known cases). This brief summary illustrates the theoretical base and the empirical background of our model.

### 3. PROPERTIES OF NUCLEUS FAR FROM THE $\beta$ -STABILITY LINE

With the macro-microscopic model and the parameters given in the above section, some of the properties of nuclei far from the  $\beta$ -stability line are studied.

(1) Variations of binding energies with proton number  $Z$ , neutron number  $N$ , and the drip lines. For simplicity, we shall leave off the microscopic corrections at first. Typical results of calculations are presented in Figs. 1 and 2. In Fig. 1, it can be seen that for fixed  $Z$ , the binding energy increases quickly with  $N$  at first. With increasing  $N$  the binding energy increases slower and slower, until the point arrives where the binding energy decreases with further increasing of neutrons and the neutron drip line is reached. In Fig. 2,  $N$  is fixed with changing  $Z$ , the changing of the binding energies follows the same pattern. In the figures, the waving zigzag of the curve arises from the average pairing effect. We have also calculated the binding energies with the finite range model (FRM) of Möller and Nix [6]. The results are plotted as dotted lines in the figures. The difference between the two models are rather small. According to the binding energy curves obtained for fixed  $Z/N$  and varying  $N/Z$ , neutron and proton drip lines can be fixed with the results shown in Fig. 3. For comparison, the results of other macroscopic model with microscopic corrections are shown in Fig. 4. On the whole the two figures are similar. Significant differences arise for nuclei near the drip lines. Close to the drip line, the binding energies change only slightly with the addition of a single nucleon, therefore even a small

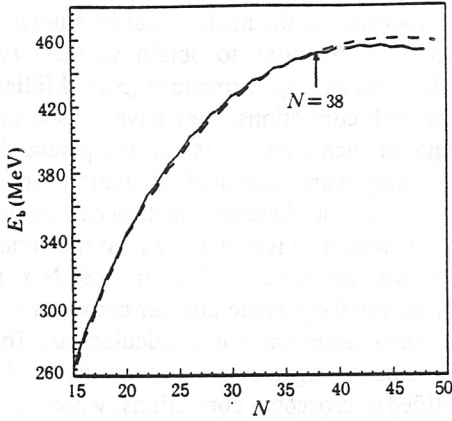


Fig. 1

Change of binding energy with  $N$  for  $Z = 20$  isotopes.

—: present model; ----: Möller.

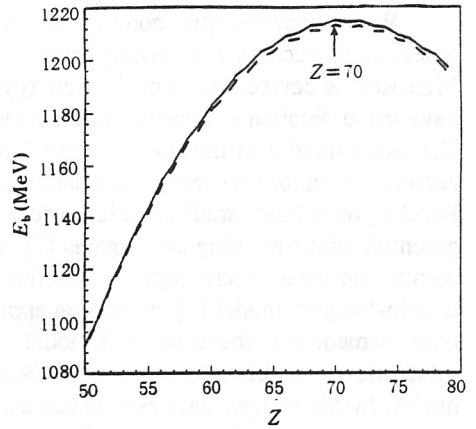


Fig. 2

Change of binding energy with  $Z$  for  $N = 82$  isotopes.

—: present model; ----: Möller.

shell correction can affect the position of the drip line. For a nucleus near the drip line, the outside nucleons are very loosely bounded; therefore, accurate microscopic corrections are required.

(2) Density distributions and nuclear radii. One of the special feature of the present model is the possibility of calculating the density distributions, which is one of the important properties of the nucleus. We have calculated the density distributions and the variation of rms radii of protons and neutrons along the isotopic lines for several spherical nuclei. Figures 5 and 6 are typical results of calculations. To reduce the Coulomb energy, the results of calculations show a slight depression of proton density in the central region, in agreement with measurements. For fixed  $Z$  (i.e., fixed total charge), proton density also changes with increasing  $N$ , decreasing of the proton density in the central region and increasing of the rms proton radius. The neutron density in the central region increases with  $N$  together with the neutron radius. However, the nuclear matter density in the central region is kept

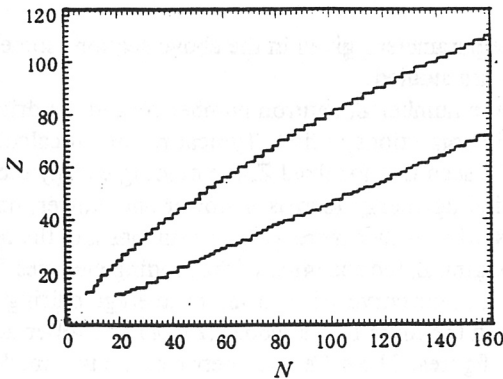


Fig. 3

Neutron and proton drip lines, microscopic corrections are not included.

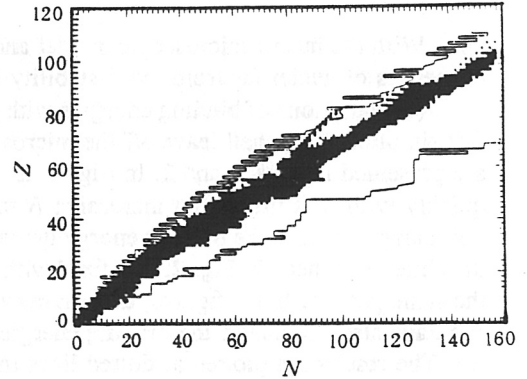


Fig. 4

Neutron and proton drip lines [8], with microscopic corrections, shaded part indicates nuclei with known masses.



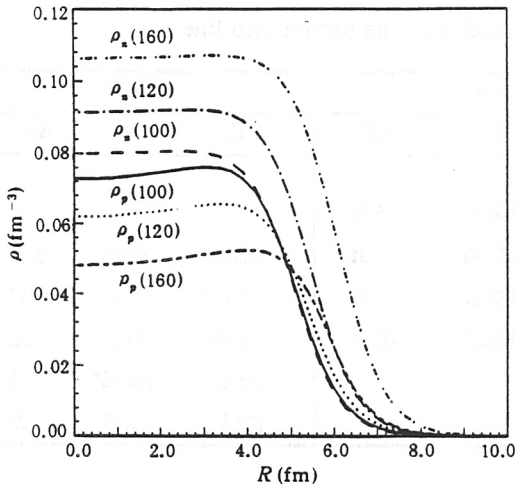


Fig. 5

Proton and neutron densities of Sn isotopes.

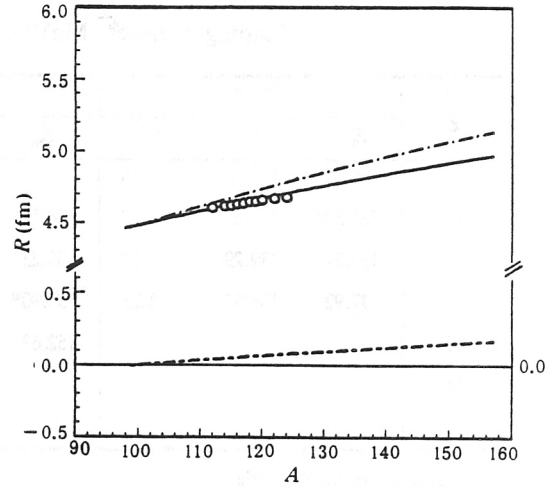


Fig. 6

Proton and neutron rms radii of Sn isotopes.

—:  $r_p$ ; ---:  $r_n$ ; ○:  $r_p$  (exp).

almost unchanged during the variation of  $N$ . It can be seen in Fig. 6, that both the proton and neutron radii increase with  $N$ , but the neutron radius increases faster, therefore a neutron skin is predicted. Compared with the results of other models, the neutron skin calculated from our model may be slightly thinner. Although the nuclear radii predicted by various models may agree well with empirical results, the region of comparison is rather narrow (for Sn isotopes, empirical values are limited to the region  $112 \leq A \leq 124$ ). Therefore, extending to the drip line may lead to larger deviations. This is an indication that experimental studies of nuclei far from the  $\beta$ -stability line may play a decisive role in the verification of different models.

(3) Proton radioactivity near the proton drip line. Experimentally, it is possible to study proton radioactivity of nuclei near the proton drip line. It may provide a check for theoretical models. In Table 1, several examples are given for the binding energies of nuclei near the proton drip line calculated with our model. In the table, binding energies calculated without microscopic corrections are denoted by  $E_{bo}$ , while those with the microscopic corrections by  $E_b$ , energy released by the capture of the last proton are denoted by  $\Delta E_p$ . For isotopes with  $N = 8$  and  $9$ , the drip line positions are the same, whether microscopic corrections are included or not. For  $N = 10$ , the drip line position changes by  $\Delta Z = 2$  when microscopic corrections are included. This is a clear indication to the necessity of inclusion of microscopic corrections for nuclei close to the drip line.

Data given in Table 1 show that proton radioactivity may exist for nuclei close to the proton drip line. Take the isotopes with  $N$  equal to 8 as an example,  $^{19}_{11}\text{Na}$  lies beyond the proton drip line ( $Z = 10$ ). However, with a  $^{17}_9\text{F}$  target, it is possible to realize a two protons transfer reaction to obtain  $^{19}_{11}\text{Na}$ . In this reaction, 1.06 MeV of energy is released.  $^{19}_{11}\text{Na}$  is unstable to proton decay, but with a sufficient life time for experimental studies, due to the Coulomb barrier. For  $N = 9$ , similar proton radioactivity may exist for  $^{22}_{13}\text{Al}$ . Experimental studies of the proton radioactivities of these nuclei may yield important nuclear structure information and provide verification of nuclear models.

(4) Comparison with other models. New experimental data are essential for the verification of nuclear models. However, due to the lack of crucial empirical data, a decisive confrontation of experimental results is impossible at present. Therefore, comparison between the results of different models is still useful.

**Table 1**  
Binding energies (MeV) of nuclei near the proton drip line.

$Z$	$N=8$			$N=9$			$N=10$		
	$E_{bo}$	$E_{bs}$	$\Delta E_1$	$E_{bo}$	$E_{bs}$	$\Delta E_1$	$E_{bo}$	$E_{bs}$	$\Delta E_1$
9	129.85	138.23	3.16						
10	136.32*	139.50*	1.27	148.11	154.09	5.56			
11	135.21	139.29	-0.21	150.23	155.90	1.81	166.39	169.98	5.12
12	137.92	138.97	-0.23	153.90*	158.57*	2.69	172.84*	173.15	3.17
13				152.63	158.27	-0.28	172.47	174.67	1.52
14							175.57	174.78*	0.11
15							172.36	173.49	-1.29

\*Position of the drip line.

**Table 2**  
Properties of Zr isotopes, comparison of the results of our model with those obtained from RMF.

	$A$	84	90	94	96	98	100	106	110
$E/u$ (MeV/u)	RMF	-8.58	-8.73	-8.64	-8.59	-8.53	-8.48	-8.27	-8.10
	This paper	-8.58	-8.74	-8.67	-8.63	-8.58	-8.53	-8.34	-8.18
	Exp	-8.55	-8.71	-8.67	-8.63	-8.58	-8.52		
$r_n$ (fm)	RMF	4.23	4.36	4.47	4.53	4.60	4.75	4.90	5.02
	This paper	4.28	4.35	4.42	4.47	4.53	4.59	4.68	4.74
	Exp								
$r_p$ (fm)	RMF	4.23	4.29	4.32	4.32	4.34	4.63	4.75	4.85
	This paper	4.27	4.31	4.36	4.40	4.46	4.50	4.58	4.63
	Exp		4.27	4.33	4.40				

$E/u$  is average binding energy per nucleon;  $r_n$  is the neutron radius, and  $r_p$  is the proton radius.

Calculations of nuclear properties for nucleons far from the  $\beta$ -stability line has been performed with FRM [6] and the droplet model [9] (DM). The binding energies and the positions of drip lines obtained are close to the results of our model. The proton distributions and the rms radii obtained from DM is also in agreement with the results of our model.

The results of our model have been compared with those obtained from the relativistic mean field theory (RMF) [10]. In Table 2, results for Zr isotopes obtained from both models are listed together with the known empirical data. On the whole, the results obtained from the two models are in close agreements and also in agreement with the empirical data. For the binding energies per nucleon, our results are in slightly better agreement with the empirical data.

(5) Exotic properties of light nuclei near the drip line. Recently, investigations of the exotic properties of light nuclei, such as  ${}^6_2\text{He}$ ,  ${}^{11}_3\text{Li}$  and  ${}^{14}_4\text{Be}$  have excited wide interest. Generally speaking, macroscopic models deal with the average behaviors of the nucleus and cannot be used to describe the behavior of one or a pair of nucleons. Therefore, the model is more suitable to describe nuclei with

many nucleons. According to our calculations, agreements with empirical data can be obtained for light nucleus such as  $^{16}_8\text{O}$ . It is not suitable to apply the model to nuclei such as  $^6_2\text{He}$ ,  $^{11}_3\text{Li}$ ,  $^{14}_4\text{Be}$  with only 2-4 protons. However, as a trial, we have calculated the proton and neutron densities, the rms radii  $r_p$  and  $r_n$  and the neutron skins of  $^{11}_3\text{Li}$  and  $^{14}_4\text{Be}$  with the following results:

$$^{11}_3\text{Li}: r_p = 2.389\text{fm}, r_n = 2.630\text{fm}, \Delta r = 0.241\text{fm}.$$

$$^{14}_4\text{Be}: r_p = 2.529\text{fm}, r_n = 2.754\text{fm}, \Delta r = 0.225\text{fm}.$$

Generally speaking, a thick neutron skin can be obtained, but quantitative results are not satisfactory. Microscopic models must be used to study the neutron halos of light nuclei.

Finally, it is to be emphasized that studies of the properties of nuclei far from the  $\beta$ -stability line are still at their very beginning. Models are to be developed and studied. New experimental data are crucial for the decisive advancement of theoretical studies.

## REFERENCES

- [1] Hu Jimin, *High Energy Phys. and Nucl. Phys.* (in Chinese), **5**(1981), p. 244.
- [2] Hu Jimin and Zheng Chunkai, *Nuclear Physics* (in Chinese), **7**(1985), p. 1.
- [3] Zheng Chunkai, *High Energy Phys. and Nucl. Phys.* (in Chinese), **14**(1990), p. 753.
- [4] Chen Xinyi and Hu Jimin, *High Energy Phys. and Nucl. Phys.* (in Chinese), **13**(1989), p. 380.
- [5] P. Möller and J.R. Nix, *Atomic Data and Nuclear Data Tables*, **26**(1981), p. 165.
- [6] P. Möller and J.R. Nix, *Atomic Data and Nuclear Data Tables*, **39**(1988), p. 213.
- [7] Hu Jimin, Zheng Chunkai, and Xu Furong, *High Energy Phys. and Nucl. Phys.* (in Chinese), **14**(1990), p. 945.
- [8] J.A. Sawicki *et al.*, *The Isospin Laboratory, Research Opportunities with Radioactive Nuclear Beams, Prepared by the North American Steering Committee for the Isospin Laboratory*, LALP 91-51, p. 49.
- [9] W.D. Myers and K.H. Schmidt, *Nucl. Phys.*, **A410**(1983), p. 61.
- [10] J.A. Sheikh and P. Ring, *Phys. Rev.*, **C47**(1993), R1850.